ISSN 0020-1685, Inorganic Materials, 2020, Vol. 56, No. 11, pp. 1127–1132. © Pleiades Publishing, Ltd., 2020.
Russian Text © The Author(s), 2020, published in Neorganicheskie Materialy, 2020, Vol. 56, No. 11, pp. 1188–1193.

Synthesis, Structure, and Properties of Titanium Diboride Nanoparticles

A. A. Vinokurov[a], D. Yu. Kovalev[b], I. I. Korobov[a], O. V. Kravchenko[a], S. V. Konovalikhin[b], N. Yu. Khomenko[b], G. V. Kalinnikov[a], S. E. Nadkhina[a], and S. P. Shilkin[a, *]

[a] *Institute of Problems of Chemical Physics, Russian Academy of Sciences, Chernogolovka, Moscow oblast, 142432 Russia*

[b] *Merzhanov Institute of Structural Macrokinetics and Materials Science, Russian Academy of Sciences, Chernogolovka, Moscow oblast, 142432 Russia*

**e-mail: ssp@icp.ac.ru*

Received March 3, 2020; revised June 19, 2020; accepted June 30, 2020

Abstract—The products of reaction between $TiCl_4$ and $NaBH_4$ in NaCl/KCl or KBr ionic melts at 973 and 1023 K under an argon pressure of 5 MPa have been characterized by various physicochemical analysis techniques. The results demonstrate that these conditions lead to the formation of TiB_2 nanoparticles with hexagonal symmetry (sp. gr. *P*6/*mmm*, AlB_2 structure) and lattice parameters $a = 0.3022–0.3025$ nm and $c = 0.3214–0.3221$ nm. The average diameters of the TiB_2 nanoparticles evaluated from electron microscopy, specific surface area, and X-ray diffraction (crystallite size) data for the two synthesis temperatures are ~10 and ~15, ~12 and ~17, and ~5 and ~10 nm, respectively.

Keywords: nanoparticle, titanium diboride, titanium tetrachloride, sodium borohydride, NaCl/KCl ionic melt, KBr, autoclave reactor

DOI: 10.1134/S0020168520110163

INTRODUCTION

Titanium diboride (TiB_2) combines a high melting point (3498 K), high hardness (≥25 GPa), high modulus of elasticity (≥450 GPa), low resistivity (10–30 Ω cm), high thermal conductivity (60–120 W/(m K)), good chemical stability and corrosion resistance in aggressive gaseous and liquid media, and low density (4.5 g/cm^3), which allows it to find effective applications in various areas of modern engineering and industry [1–5]. Recent years have seen a considerable increase of interest in titanium diboride and related compounds because they have been used as basic components for producing nanomaterials with various and excellent physicochemical, mechanical, and other properties, differing significantly from the properties of their microcrystalline analogs (see, for example, Refs. [6, 7]).

Titanium diboride nanoparticles can be prepared via the thermolysis of titanium borohydride derivatives at a temperature of ~488 K [8, 9], for example, according to the scheme

$$Ti(BH_4)_3 \cdot nSolv \xrightarrow{t} TiB_2 + 0.5B_2H_6 + 4.5H_2 + nSolv \quad (1)$$

where *Solv* stands for dimethoxyethane, tetrahydrofuran, diglyme, triglyme, etc. The TiB_2 prepared according to this scheme in the form of powder or film is X-ray amorphous and crystallizes in vacuum after annealing between 1173 and 1273 K. However, the described process takes a considerable time and is multistep, so the resultant TiB_2 is contaminated with appreciable amounts of carbon and oxygen. TiB_2 nanoparticles can also be prepared through mechanochemical interaction of titanium(III) chloride with lithium hydride and lithium borohydride in a high-energy mill according to the reaction scheme [10]

$$TiCl_3 + 2LiBH_4 + LiH \xrightarrow{t} TiB_2 + 3LiCl + 4.5H_2. \quad (2)$$

Pan et al. [11] obtained TiB_2 with a crystallite size of a few nanometers via ~873-K heat treatment of a $LiBH_4 + TiO_2$ mixture preactivated in a high-energy mill. In addition, TiB_2 nanoparticles can be prepared through mechanochemical interaction of microcrystalline titanium and boron in a high-energy mill [12]. Moreover, titanium diboride nanoparticles can be obtained by reacting sodium borohydride with $TiCl_4$ at elevated temperatures and pressures [13, 14] or by reacting Ti with BBr_3 in the presence of sodium at 673 K [15] and by a carbothermic process [16] according to the reaction scheme

$$TiO_2 + B_2O_3 + 5C \xrightarrow{t} TiB_2 + 5CO, \quad (3)$$

as well as via magnesiothermic reduction of mixtures of titanium and boron oxides in a NaCl/KCl melt [17]. Besides, titanium diboride nanoparticles can be prepared by reacting boron and titanium powders in a $Na_2B_4O_7$ ionic melt [18].

Each of the above techniques has its advantages and drawbacks. Some of them make it possible to obtain nanoparticles with low impurity concentrations but at a slow rate; others ensure the formation of titanium diboride nanoparticles with the stoichiometric composition and tailored size at relatively low temperatures, but require sophisticated apparatus, etc.

The objectives of this work were to examine the feasibility of formation of TiB_2 nanoparticles via heterophase interaction of $TiCl_4$ with $NaBH_4$ in NaCl/KCl or KBr ionic melts and investigate their physicochemical properties.

EXPERIMENTAL

Starting chemicals. Sodium borohydride of 99.5+% purity was prepared through recrystallization of a crude substance from a 1 N NaOH solution and dried under a vacuum of 0.133 Pa at 373 K. In addition, we used off-the-shelf OTT-O $TiCl_4$, which was vacuum-distilled over copper turnings before synthesis; reagent-grade KCl, NaCl, and KBr; and high-purity (99.998%) argon (Russian Federation Purity Standard TU 2114-005-0024760-99). As a source of 99.999+%-pure hydrogen, we used a self-contained laboratory-scale hydrogen generator containing hydrided $LaNi_5$ and TiFe intermetallic phases as working materials. Its operating principle was described in detail previously [19, 20].

Characterization techniques. The phase composition of the synthesized TiB_2 nanoparticles was determined by X-ray diffraction on a DRON-3 diffractometer (diffracted-beam monochromator). X-ray diffraction patterns were collected in step scan mode with CuK_α radiation in the angular range $2\theta = 20°–90°$, with a scan step of 0.02° and a counting time per data point of 4 s. In X-ray diffraction data processing by the profile analysis method, we used Burevestnik software. Unit-cell and fine-structure parameters were evaluated using eight reflections. Instrumental broadening was assessed from the linewidth of a LaB_6 reference standard (SRM 660b). The average crystallite (coherent scattering domain) size D was evaluated using the method of second moments.

The thermal properties of the nanoparticles were studied by simultaneous thermal analysis in a Netzsch STA 409 PC Luxx thermoanalytical system in combination with a QMS 403 C Aëolos quadrupole mass spectrometer at a constant heating rate of 10 K/min under flowing argon in the temperature range from 293 to 1273 K.

The powders were also examined by electron microscopy and energy dispersive X-ray analysis on a Zeiss Supra 25 field emission scanning electron microscope equipped with an INCA x-sight X-ray spectrometer system. Electron micrographs were obtained at low electron beam accelerating voltages (~4 kV). At such accelerating voltages, the contribution of the substrate to the measured signal was negligible, if any. Energy dispersive X-ray analysis was carried out at an accelerating voltage of ~8 kV.

To more accurately determine the qualitative surface composition of the titanium diboride powders, we measured their X-ray photoelectron spectra on a PHOIBOS 150 MCD electron spectrometer system. The specific surface area (S) of the samples was determined by BET analysis of krypton adsorption data obtained at liquid-nitrogen temperature after removing volatile impurities from the solid phase under a vacuum of 1.3×10^{-3} Pa at a temperature of 373 K. The cross-sectional area of an adsorbed krypton atom was taken to be 19.5×10^{-20} m^2. The relative error of determination was within ±10%. From the S measurement results, we evaluated the average particle size of TiB_2 under the assumption that the particles were spherical in shape, using the well-known formula $d_x = 6/(\gamma S)$, where d_x is the particle size and γ is X-ray density.

Boron, titanium, chloride and bromide ions, and oxygen were determined by standard analytical techniques and energy dispersive X-ray analysis. Hydrogen was determined using a CHNS/O Vario EL cube Elementar analyzer. The pressure in the system was measured with certified reference manometers of accuracy class 0.4.

Experimental procedure. $TiCl_4$ was reacted with $NaBH_4$ in NaCl/KCl or KBr ionic melts as follows: A silica ampule containing titanium tetrachloride, sodium borohydride, and a 50 mol % NaCl + 50 mol % KCl or KBr eutectic mixture was placed in a stainless steel autoclave reactor under a high-purity argon atmosphere. Next, the autoclave reactor was cooled to 173 K, evacuated for 5 min, filled with argon at a pressure of 5 MPa, and heated for a predetermined time at a temperature of 973 or 1023 K. The reaction temperatures (973 and 1023 K) were chosen based on the melting points of the 50 mol % NaCl + 50 mol % KCl (931 K) or KBr (1007 K) eutectic. The argon pressure in the autoclave reactor, 5 MPa, was above the critical pressure for $TiCl_4$ ($p_c = 4.57$ MPa), and $NaBH_4$ was added in large excess with respect to $TiCl_4$ (1 : 10 molar ratio).

Next, the reactor was cooled to room temperature, and the reaction products were evacuated for an additional 0.5 h. After the reactor was opened under an argon atmosphere, the reaction products were washed sequentially with cooled distilled water, acetone, and ethanol and then held for 5–6 h at 313 K and a residual vacuum of 0.13 Pa. Next, the resultant powder was

Table 1. Conditions and results of reaction between $TiCl_4$ and $NaBH_4$ in a NaCl/KCl or KBr ionic melt and without it

Phase composition of the reaction products	*a*, nm	*c*, nm	Synthesis temperature, K	Synthesis time, h	Ionic melt
TiB_2 [13]*	0.3032	0.3229	973	12	–
TiB_2 [14]*	0.3027	0.3213	1020	10	–
TiB_2	0.3023	0.3214	973	7	NaCl/KCl
TiB_2	0.3022	0.3221	1023	5	NaCl/KCl
TiB_2	0.3025	0.3215	1023	5	KBr

* $TiCl_4$ was reacted with $NaBH_4$ with no NaCl/KCl of KBr ionic melt.

again placed in the reactor, exposed to flowing hydrogen from a hydrogen storage alloy at a pressure of 5 MPa and temperature of 373 K as described by Fokin et al. [21], again pumped down to a residual pressure of 0.133 Pa at room temperature, and withdrawn from the reactor under an argon atmosphere.

RESULTS AND DISCUSSION

Table 1 summarizes our results on reaction between $TiCl_4$ and $NaBH_4$ in NaCl/KCl or KBr ionic melts under an argon pressure at a reaction time from 5 to 7 h. According to the chemical and energy dispersive X-ray analysis data, the synthesized titanium diboride had the composition $TiB_{2.0–2.02}O_{0.01–0.03}$, without detectable amounts of chloride or bromide ions or hydrogen. According to X-ray diffraction characterization results, the titanium diboride nanoparticles have hexagonal symmetry (sp. gr. *P*6/*mmm*, AlB_2 structure) (Fig. 1a). Their lattice parameters (Table 1) are consistent with data reported in Refs. [13–15, 18] and agree with the lattice parameters indicated in the ICDD PDF-2 X-ray diffraction database (Fig. 1b). We did not detect any significant amounts of impurity phases.

The thermal analysis, X-ray diffraction, and electron microscopy data showed that, during heating in an argon atmosphere from 293 to 1273 K, the titanium diboride nanoparticles prepared as described above did not undergo any noticeable transformations related to heat release or absorption, nor did we detect any changes in particle weight, size, or shape, lattice parameters, or crystallite size. This points to high thermal stability of the nanoparticles.

Table 2 compares the average TiB_2 particle diameters evaluated from the present electron microscopy and X-ray diffraction data and specific surface area measurement results. Figure 2 shows electron micrographs of TiB_2 powder particles obtained at 973 (Fig. 2a) and 1023 K (Fig. 2b) in a NaCl/KCl ionic melt and at 1023 K in a KBr ionic melt (Fig. 2c). According to the scanning electron microscopy data, the titanium diboride particles synthesized at temperatures of 973 and 1023 K in NaCl/KCl and KBr ionic melts were not splintery in shape but nearly spherical, characteristic of compounds obtained as a result of a chemical reaction. The average particle size of TiB_2 evaluated from the electron microscopy data agrees well with the equivalent TiB_2 particle diameter determined from the measured specific surface area of the TiB_2 powder by the BET method (Table 2). With increasing synthesis temperature, the particle size of TiB_2 increases. The synthesized TiB_2 nanopowders were predominantly aggregated.

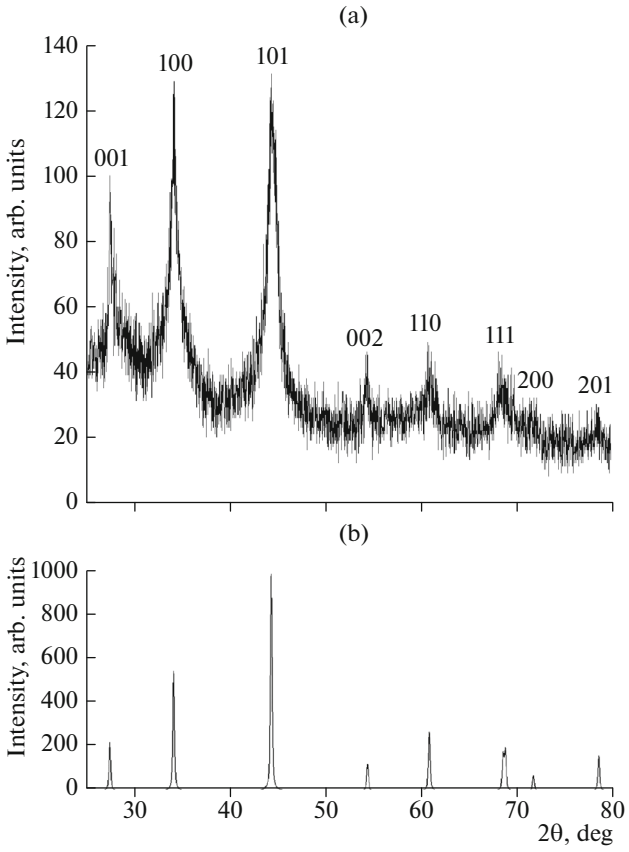

Fig. 1. (a) X-ray diffraction pattern of the TiB_2 powder nanoparticles and (b) ICDD PDF-2 data (card no. 000-35-0741).

Table 2. Average diameter of TiB_2 particles prepared by reacting $TiCl_4$ with $NaBH_4$ in a NaCl/KCl or KBr ionic melt or with no melt at temperatures of 973 and 1023 K

Synthesis temperature, K	Average particle diameter from electron microscopy data, nm	D, nm	Average particle diameter from specific surface data, nm
973	~10	~5	~12 (S = 115 m^2/g)
1023	~14	~7	~17 (S = 80 m^2/g)
1023	~15	~10	~16 (S = 82 m^2/g)
973* [13]	10–20	–	–
1020* [14]	35–50	~ 30	~45 (S = 30 m^2/g)

* $TiCl_4$ was reacted with $NaBH_4$ with no NaCl/KCl of KBr ionic melt.

Table 3. Calculated thermodynamic parameters of reactions (4) and (5) in the temperature range 623–1073 K

T, K	ΔH, kJ/mol	ΔS, J/(mol K)	ΔG, kJ/mol	ΔH, kJ/mol	ΔS, J/(mol K)	ΔG, kJ/mol
	(4)			(5)		
623	–135.8	390.4	–379.0	104.6	399.1	–144.0
673	–135.8	390.3	–398.5	103.7	397.7	–163.9
723	–136.0	390.0	–418.0	102.7	396.3	–183.8
773	–136.3	389.7	–437.5	101.9	395.2	–203.6
823	–136.5	389.3	–457.0	101.1	394.2	–223.3
873	–136.8	389.0	–476.4	100.5	393.4	–243.0
923	–137.0	388.8	–495.9	99.9	392.9	–262.7
973	–137.2	388.6	–515.3	99.6	392.5	–282.3
1023	–137.2	388.6	–534.7	99.5	392.4	–301.9
1073	–137.1	388.7	–554.2	99.5	392.4	–321.5

To more accurately determine the qualitative surface composition of the TiB_2 nanoparticles, we measured their X-ray photoelectron spectra. Along with lines characteristic of titanium diboride (187.5–187.7 eV, B 1*s*; 454.2–454.4 eV, Ti $2p_{3/2}$), there were weak lines corresponding to boron and titanium oxides (193.7–193.8, 463.2–463.3, and 468.7–468.2 eV), in agreement with data in the literature.

The novelty of the proposed TiB_2 synthesis process is that $TiCl_4$ and $NaBH_4$ are reacted in an ionic melt. Compared to reaction between $TiCl_4$ and $NaBH_4$ with no ionic melt, this makes it possible to reduce the synthesis time and obtain smaller TiB_2 nanoparticles without their consolidation at high temperatures of reaction between starting chemicals, which is prevented by the presence of a NaCl/KCl or KBr melt.

Chen et al. [13] proposed a feasible reaction for the formation of titanium diboride nanoparticles in the temperature range 773–973 K:

$$TiCl_4 + 2NaBH_4 = TiB_2 + 2NaCl + 2HCl + 3H_2. \quad (4)$$

Below 723 K, $TiCl_4$ and $NaBH_4$ seem to react according to the scheme

$$2TiCl_4 + 2NaBH_4 = TiB_2 + TiH_2 + 2NaCl + 6HCl. \quad (5)$$

We calculated thermodynamic parameters of reactions (4) and (5) in the temperature range 623–1073 K (Table 3). In our calculations, we used reference data [22]. It follows from the calculation results that the heat effect and entropy of reactions (4) and (5) are essentially independent of temperature and that reaction (4) is exothermic, whereas reaction (5) is endothermic. The calculated Gibbs energies of these reac-

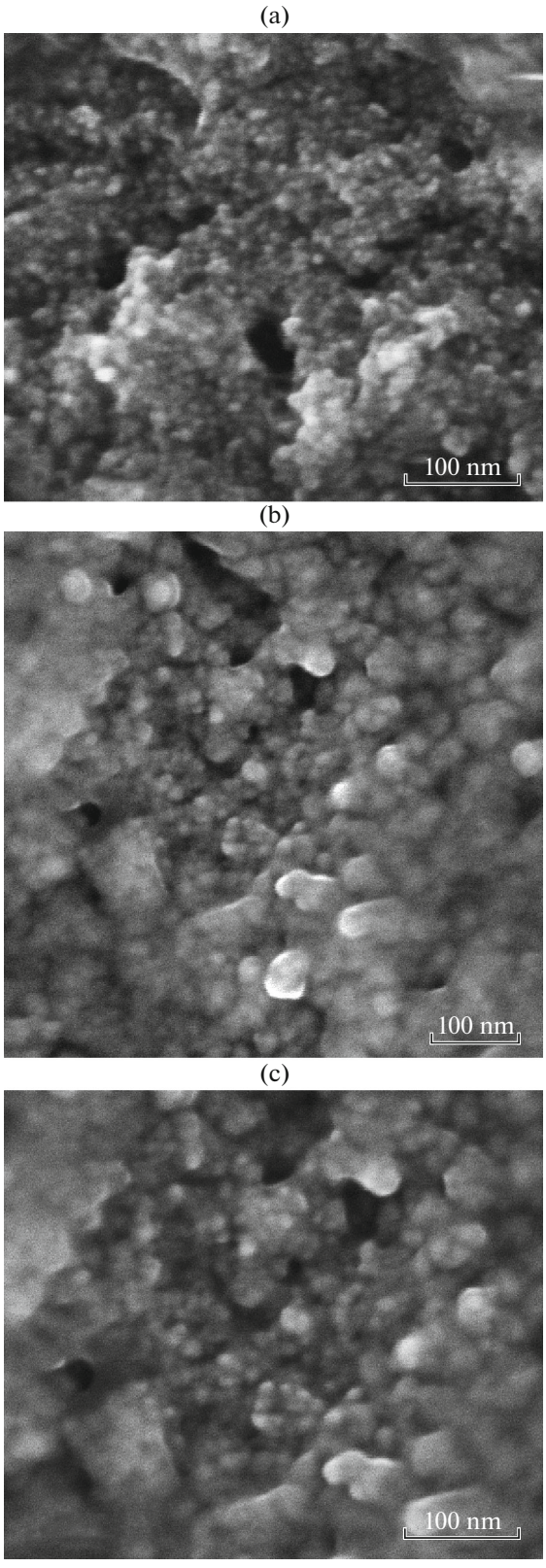

Fig. 2. Electron micrographs of TiB_2 powder nanoparticles obtained at (a) 973 and (b) 1023 K in a NaCl/KCl ionic melt and (c) at 1023 K in a KBr ionic melt.

tions suggest that reaction (4) in the temperature range in question is more energetically favorable and more likely than reaction (5).

CONCLUSIONS

The products of reaction between $TiCl_4$ and $NaBH_4$ in NaCl/KCl or KBr ionic melts at 973 and 1023 K under an argon pressure of 5 MPa have been characterized by X-ray diffraction, scanning electron microscopy, X-ray photoelectron spectroscopy, thermal analysis, energy dispersive X-ray analysis, elemental analysis, and specific surface area measurements. The results demonstrate that these conditions lead to the formation of TiB_2 nanoparticles with hexagonal symmetry (sp. gr. $P6/mmm$, AlB_2 structure) and lattice parameters $a = 0.3022–0.3025$ nm and $c = 0.3214–0.3221$ nm. The average diameters of the TiB_2 nanoparticles evaluated from the electron microscopy, specific surface area, and X-ray diffraction data for the two synthesis temperatures are ~10 and ~15, ~12 and ~17, and ~5 and ~10 nm, respectively.

FUNDING

This work was supported by the Russian Federation Ministry of Science and Higher Education, state research targets for the Institute of Problems of Chemical Physics, Russian Academy of Sciences (theme state registration no. AAAA-A19-119061890019-5) and the Merzhanov Institute of Structural Macrokinetics and Materials Science, Russian Academy of Sciences (theme no. 44.1).

ACKNOWLEDGMENTS

In this study, we used equipment at the Shared Analytical Facilities Center, Institute of Problems of Chemical Physics, Russian Academy of Sciences.

REFERENCES

1. Berger, M., Hogmark, S., Karlsson, L., and Larsson, M., Low stress TiB_2 coatings with improved tribological properties, *Thin Solid Films,* 2001, vol. 401, nos. 1–2, pp. 179–186.
2. Agarwal, A. and Dahotre, N.B., Laser surface engineering of steel for hard refractory ceramic composite coating, *Int. J. Refract. Met. Hard Mater.,* 1999, vol. 17, pp. 283–293.
3. Cardarelli, F., *Material Handbook,* Charm: Springer, 2018, pp. 936–937.
4. Efimova, K.A., Galevskii, G.V., and Rudneva, V.V., Current status of titanium diboride production: evaluation, predominant trends, and future prospects, *Nauchno-Tekh. Vedomosti SPbPU. Estestv. Inzh. Nauki,* 2017, vol. 23, no. 2, pp. 144–158. https://doi.org/10.18721/JEST.230213
5. Samsonov, G.V., Serebryakova, T.I., and Neronov, V.A., *Boridy (Borides)*, Moscow: Atomizdat, 1975.

6. Andrievski, R.A. and Khatchoyan, A.V., Nanomaterials in Extreme Environments, Fundamentals and Applications. Berlin: Springer, 2016. https://doi.org/10.1007/978-3-319-25331-2
7. Andrievskii, R.A., Nanostructured titanium, zirconium, and hafnium diborides: synthesis, properties, size effects, and stability, *Usp. Khim.,* 2015, vol. 84, no. 5, pp. 540–554. https://doi.org/10.1070/RCR4469
8. Jensen, J.A., Gozum, J.E., Pollina, D.M., and Girolami, G.S., Titanium, zirconium and hafnium tetrahydroborates as "tailored" CVD precursors for metal diboride thin films, *J. Am. Chem. Soc.,* 1988, vol. 110, no. 5, pp. 1643–1644. https://doi.org/10.1021/ja00213a058
9. Andrievski, R.A., Kalinnikov, G.V., Kravchenko, S.E., Tarasov, B.P., and Shilkin, S.P., Synthesis of boride ultrafine powders and films, *Abstracts Papers Am. Chem. Soc.,* 1995, vol. 210, p. 156-PMSE (2).
10. Kim, J.W., Shim, J.-H., Ahn, J.-P., Cho, Y.W., Kim, J.-H., and Oh, K.H., Mechanochemical synthesis and characterization of TiB_2 and VB_2 nanopowders, *Mater. Lett.,* 2008, vol. 62, pp. 2461–2464. https://doi.org/10.1016/j.matlet.2007.12.022
11. Pan, W.Y., Qian, W.B., Mao, Y.J., Liu, B.H., and Li, Z.P., Low-temperature synthesis of nanosized metal borides through reaction of lithium borohydride with metal hydroxides or oxides, *J. Alloys Compd.,* 2015, vol. 651, pp. 661–672. https://doi.org/10.1016/j.jallcom.2015.08.149
12. Tang, W.M., Zheng, Z.X., Wu, Y.C., Wang, J.M., Lű, J., and Liu, J.W., Synthesis of TiB_2 nanocrystalline powder by mechanical alloying, *Trans. Nonferrous Met. Soc. China,* 2006, vol. 16, pp. 613–617.
13. Chen, L., Gu, Y., Qian, Y., Chi, L., Yang, Z., and Ma, J., A facile one-step route to nanocrystalline TiB_2 powders, *Mater. Res. Bull.,* 2004, vol. 39, pp. 609–613. https://doi.org/10.1016/j.materresbull.2003.12.005
14. Kravchenko, S.E., Torbov, V.I., and Shilkin, S.P., Preparation of titanium diboride nanopowder, *Inorg. Mater.,* 2010, vol. 46, no. 6, pp. 614–616.
15. Chen, L., Gu, Y., Shi, L., Yang, Z., Ma, J., and Qian, Y., A Reduction–boronation route to nanocrystalline titanium diboride, *Solid State Commun.,* 2004, vol. 130, pp. 231–233. https://doi.org/10.1016/j.ssc.2004.01.037
16. Gorlanov, E.S., Bazhin, V.Yu., and Fedorov, S.N., Carbothermic synthesis of titanium diboride: upgrade, *J. Sib. Fed. Univ. Chem.,* 2018, vol. 11, no. 2, pp. 156–166. https://doi.org/10.17516/1998-2836-0065
17. Javadi, A., Pan, S., Cao, C., Yao, G., and Li, X., Facile synthesis of 10 nm surface clean TiB_2 nanoparticles, *Mater. Lett.,* 2018, vol. 229, pp. 107–110. https://doi.org/10.1016/j.matlet.2018.06.054
18. Volkova, L.S., Shulga, Yu.M., and Shilkin, S.P., Synthesis of nano-sized titanium diboride in a melt of anhydrous sodium tetraborate, *Russ. J. Gen. Chem.,* 2012, vol. 82, no. 5, pp. 819–821.
19. Fokin, V.N., Fokina, E.E., and Shilkin, S.P., Synthesis of coarsely crystalline metal hydrides, *Russ. J. Gen. Chem.,* 1996, vol. 66, no. 8, pp. 1210–1212.
20. Fokin, V.N., Fokina, E.E., Tarasov, B.P., and Shilkin, S.P., Synthesis of the tetragonal titanium dihydride in ultradispersed state, *Int. J. Hydrogen Energy,* 1999, vol. 24, nos. 2–3, pp. 111–114. https://doi.org/10.1016/S0360-3199(98)00070-6
21. Fokin, V.N., Troitskaya, S.L., Shilkin, S.P., Fokina, E.E., and Rumynskaya, Z.A., Reaction of titanium hydride with oxygen, *Zh. Obshch. Khim.,* 1992, vol. 62, no. 8, pp. 1719–1725.22. *NIST–JANAF Thermochemical Tables,* 1998. https://doi.org/10.18434/T42S31

Translated by O. Tsarev